# River Discharge and Saltwater Intrusion Level Study of Yangtze River Estuary, China

**Zhi Xu [1,2]** , **Jing Ma [2,*]**, **Hao Wang [1,2]**, **Yajie Hu [2]**, **Guiyu Yang [2] and Wei Deng [1,2]**

[1]  Department of Hyraulic Engineering, Tsinghua University, Beijing 100084, China;
    xuzhitc159@163.com (Z.X.); wanghao@iwhr.com (H.W.); dwsylar@163.com (W.D.)
[2]  China Institute of Water Resources and Hydropower Research, Beijing 100038, China;
    huyj118@163.com (Y.H.); guiyuy@iwhr.com (G.Y.)
*  Correspondence: jingma@iwhr.com; Tel.: +86-010-68785706

check for updates

**Abstract:** The Yangtze River Estuary (YRE) is the largest estuary in China, with three-order bifurcations and four outlets into the sea. In recent years, issues of saltwater intrusions have received increased attention due to the increased levels and frequencies of the intrusions. The saltwater intrusions into the YRE resulting from river discharges were investigated in this study based on river discharge levels at the Datong station. A hydrodynamic and salinity transport model (MIKE21) was used to quantify the influences of the river discharges on the saltwater intrusions in the YRE. The model was effectively validated through observational data of the tidal and salinity levels. The 25%, 50% and 70% frequencies of the river discharges during the dry seasons were determined to be 18,112, 16,331 and 14,832 $m^3/s$, respectively. A multi-year averaged river discharge of 27,856 $m^3/s$ was used to simulate the salinity level changes resulting from the different river discharges. The results revealed the following: (1) the salinity of the South Branch (SB) was distributed as "high–low–high"; and the changes in the salinity levels were greatly affected by the river discharges. A strong correlation was found between the salinity and flow in the North Branch (NB) and SB of between 0.917 and 1; (2) the changes in the river discharges had major impacts on the changes in the salinity levels in the SB. When the runoff was 27,856 $m^3/s$, the salinity excessive area rate (the ratio between salinity excessive area (>0.45‰) and the SB area) less than 10%. However, when the river discharges were reduced to 16,331 $m^3/s$, the salinity excessive area rate is more than 50%; (3) As the river discharges decreased, the amplification line (0.2‰) also rapidly decreased, and the amplification lines (0.45‰, 2‰) increased. At points far from the river's entrance, the effects of the runoff were observed to be weakened, such as the amplification lines gradually becoming reduced; (4) the changes in the river discharges were observed to have significant impacts on the freshwater reservoir water withdrawal. When the river discharges were maintained at 27,856 $m^3/s$, the salinity of the Baogang, Chenhang, and Qingcaosha Reservoirs remained below 0.45‰. The salinity levels of the four reservoir locations examined in this study were found to exceed the Chinese drinking water standard (0.45‰) for more than 23 days in the 14,832 $m^3/s$ river discharge scenario, which negatively affected the drinking water of the population living near the YRE.

**Keywords:** river discharge; saltwater intrusion; MIKE21; Yangtze River Estuary; freshwater reservoir

## 1. Introduction

As intersections of the ocean and rivers, estuarine regions contain rich freshwater and ecological resources, as well as geographical advantages. Therefore, they have become major areas for rapid economic development and progress. At the same time, as the impacts of human activities intensify, the utilization of water resources continues to increase, and the inflow of many rivers into the sea

have been declining [1]. In particular, the durations of small discharges during dry seasons have been increasing, with some rivers even having no current flow. The balances between fresh water and saltwater which have formed over long periods of time have been broken [2]. The saltwater intrusion disasters not only have negative impacts on the human populations of the affected areas, but also endanger aquatic animals and plants [3] and destroy local fragile ecological environments. For quite some time, the estuaries of countries throughout the world have been affected by saltwater intrusion, particularly in the United States, Germany, Italy, Britain, China, and other countries with abundant estuary areas. Saltwater intrusions into these estuaries has caused enormous losses each year [4].

River discharges are restricted by many factors such as climate change, human activities, and forest coverage rates. Chen et al. (2009) examined the impacts of climate change and human activities on the river discharge of the Gushanchuan Basin, with the proportions of 72.7% and 27.3%, respectively [5]. With the exceptions of arid and semi-arid regions, increases in forested areas generally result in increased river discharge. Changes in the discharges of rivers may also cause changes in the geography and stability of river channels [6]. Furthermore, changes in river discharges impact the sea levels in estuaries. The sea levels tend to rise as river discharges decrease, and its amplification will decrease from upstream to offshore [7]. Increases in river discharge push the isohaline (0.45 psu) down-estuary, and decreases in river discharge tend to drag the isohaline up-estuary. The effects of river discharge on saltwater intrusion appear on both the horizontal and vertical of the horizontal plane, where both the saltwater intrusion distance and river flow rates are low. In the vertical direction, the river flow has greater influence on the surface layers than the bottom layers.

As the largest estuary in China, the YRE has been the focus of many saltwater intrusion research studies. The saltwater intrusions of the YRE have been studied in depth since the 1980s, and more prominently in recent years, as a result of increases in the saltwater intrusions' levels and frequency. For example, numerical simulations of the Yangtze River Estuary salinity have been performed [8–11]. The impacts of freshwater resources have also been studied [2]. Also, previous studies have been conducted regarding saltwater intrusion and the utilization of freshwater resources in the Yangtze Estuary [12]. Research was completed regarding the effect of extremely low level runoff on the saltwater intrusion at YRE was completed during extreme drought years [13]. It has been determined that the tide and river discharge have the greatest effects and are the major influencing factors in the YRE. Chen Jiyu (1995) showed that when a station's total capacity was less than 10,000 m$^3$/s, saltwater intrusions would have significant impacts on the freshwater resources in the southern branch of the Yangtze River [14]. Also, using a mathematical model, Chen Jing (2014) proposed that the saltwater intrusions on the surface and bottom of the Qingcaosha Reservoir intake mainly originated from the intrusion of saltwater in the North Branch (NB) of the river [15]. Chen Li (2013) established a model to predict the saltwater intrusion in the Chenhang Reservoir of the Yangtze River estuary using statistical laws [16].

The improvements which have been made in this study over previous investigation attempts include the following: (1) an unstructured mesh with a high resolution was applied which better fits the shoreline areas; (2) the influences of Hangzhou Bay were considered; and (3) the use of spatially varying bottom roughness was included in the experimental process. In this study, the main focus was on the effects of the river discharge on the saltwater intrusions in the YRE as well as the nearby offshore sea areas. First, a hydrodynamic and salinity transport model of the YRE was setup with a MIKE21 model. Then, the tidal levels which had been measured in situ were employed to validate the model. The characteristic averaged river discharge during the dry seasons from 1957 to 2015 were then applied to simulate sea-level changes and salinity transport process. Next, the influences of the river discharge variations on the salinity measurement stations in the YRE were studied, and the correlation between the salinity and sea discharge was analyzed. The current study also analyzed the spatial distribution of the salinity, as well as the salinity amplification lines. Finally, the effects of the river discharge on the freshwater reservoirs were quantificationally analyzed.

## 2. Data and Methodology

### 2.1. Overview of the Yangtze River Estuary (YRE)

The Yangtze River Estuary is China's most populated and industrially productive area. The country's four major drinking-water reservoirs (Qingcaosha, Baogang, Chen Hang, and Dongfeng Xisha Reservoirs) are located in the YRE (Figure 1). These reservoirs provide abundant water sources for the cities in the estuary area, including those of Jiangsu Province and Shanghai Municipality.

The Dongfeng Xisha Reservoir is located on the north side of the upper reach of the SB, with a total capacity of up to 9.762 million m$^3$. The Baogang Reservoir is located at the south bank of the SB. Its storage volume has been decreased due to sedimentation in the reservoir. The Chenhang Reservoir is located in the downstream area of Lihekou and has a comparatively small capacity. The Qingcaosha Reservoir, which is located in the northern part of Changxing Island, has an area of 70 km$^2$, and a capacity of 0.44 billion m$^3$. The water quality in the Qingcaosha Reservoir is considered to be very high (Category I or II) according to Chinese surface water standards, which makes the Qingcaosha Reservoir one of the most efficient reservoirs in China at this time.
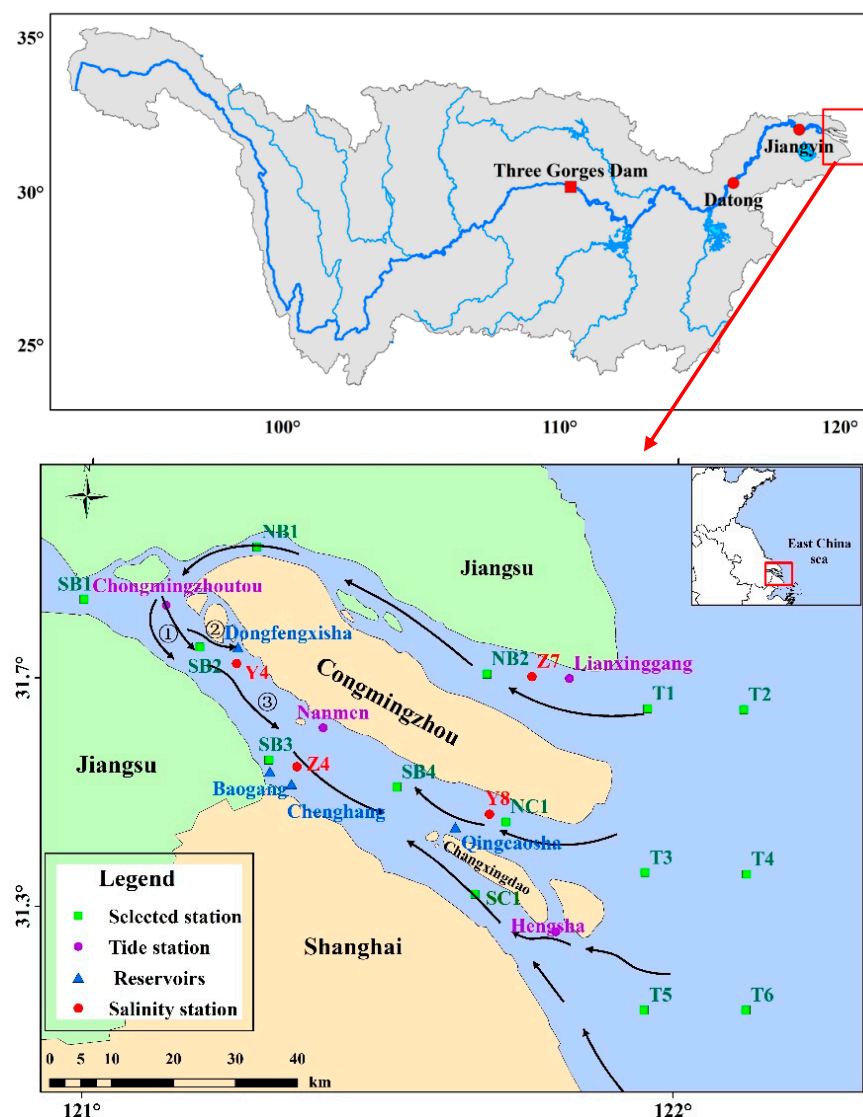


**Figure 1.** The range of the Yangtze River Estuary (YRE).

The saltwater intrusion path of the YRE has been determined to be as follows: The upper section of the North Branch of the YRE has a trumpet-shaped topography, resulting in an only 5% runoff into the sea, and the branch's access being located far offshore [12]. In particular, during the dry seasons, the high-salinity water in the NB of the YRE can reach as far as Qinglonggang Harbor. The tides of the NB may rise across to Chongming Island and head into the SB of the YRE. The South Branch (SB) and NB then become inundated, as shown in Figure 1. The lower part of the SB will be then be mainly affected by the ocean tides and form a saltwater intrusion path inward from the river's mouth.

*2.2. River Discharge*

The Yangtze River is the longest river in China, with a total length of 6380 km. Its catchment area measures $1.8 \times 10^6$ km$^2$. Its annual mean freshwater discharge of 27,856 m$^3$/s was obtained using measurements recorded from 1957 to 2015 at the Datong hydrological station. The discharge has been observed to have obvious seasonal changes (Figure 2). During the dry seasons each year (November to April) the discharge averages approximately 16,542 m$^3$/s. The construction of the Three Gorges Dam redistributed the annual discharge into the middle and lower reaches of the Yangtze River. The Three Gorges Dam was built in 1994 and completed in 2009. As of the end of September 2006, the flood control capacity of the Three Gorges Reservoir began to play a role in the flood seasons. Therefore, the distribution of the yearly discharge into the middle and lower reaches of the Yangtze River was determined to have changed after 2006 (Table 1).
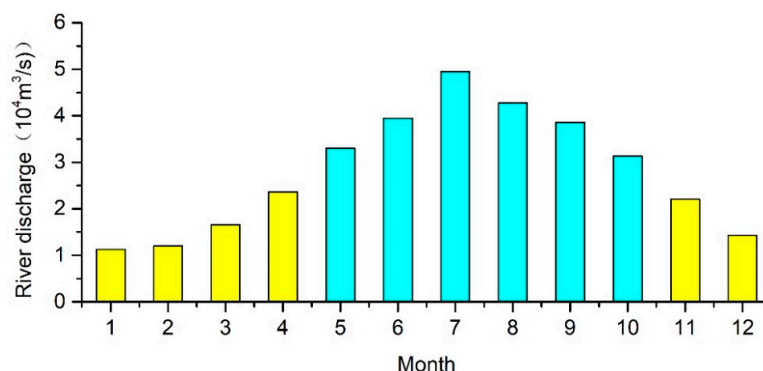


**Figure 2.** Annual runoff distribution process of Datong hydrological station for 1957–2015 years.

**Table 1.** Annual discharge characteristics before and after the establishment of the Three Gorges Dam.

| Time | Flood Season | | Dry Season | |
|------|---------------------------|--------------------------|---------------------------|--------------------------|
| | Annual Discharge/(m$^3$/s) | Distribution Rate (%) | Annual Discharge/(m$^3$/s) | Distribution Rate (%) |
| 1957–2005 | 39,799 | 70.64% | 16,541 | 29.36% |
| 2006–2015 | 35,579 | 68.26% | 16,543 | 31.74% |

The average annual discharge of Datong hydrological station from 2006 to 2015 was 10.6% lower than the average flow from 1957 to 2005. Also, the annual distribution rate of the discharge had decreased by 2.4%. The average annual runoff during dry seasons basically remained unchanged. However, the distribution rate of discharge had increased by 2.4%.

In this study, a Pearson III (P-III) frequency curve was used to analyze the monthly river discharges documented at the Datong station spanning from 1957 to 2015 [7]. The statistical analysis results obtained for the 25%, 50%, and 75% frequency of river discharges were 18,112, 16,331 and 14,832 m$^3$/s, respectively, during the dry seasons (Figure 3). The multi-year average of the river discharges was approximately 27,856 m$^3$/s during the dry seasons, where the fitting curve displayed a variation coefficient (Cv) of 0.13, and a deviation coefficient (Cs) of 0.65.
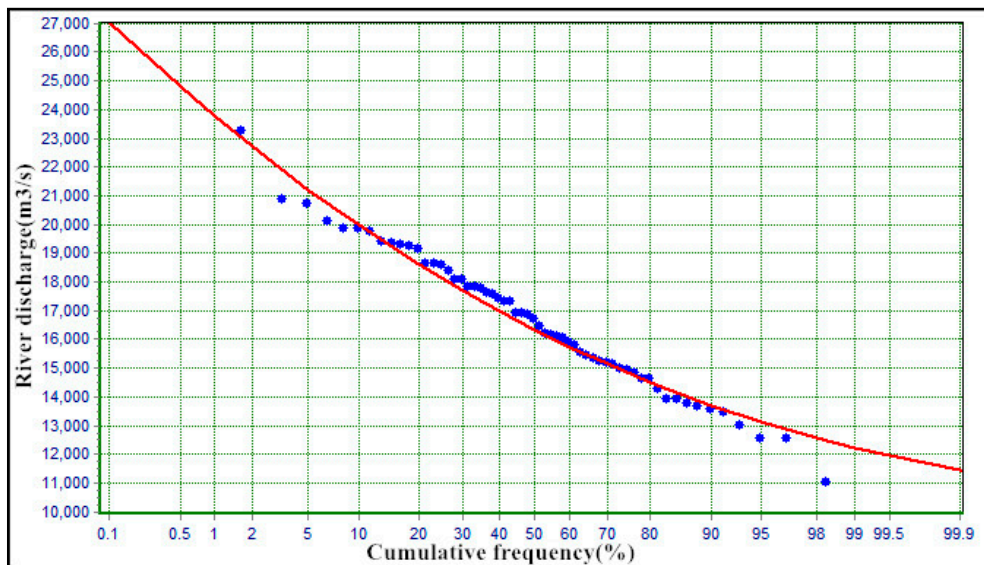
**Figure 3.** Cumulative frequency curve of river discharges in the dry season at the Datong station from 1957 to 2015.

## 2.3. Numerical Model

In the current study, a MIKE21 model [17] developed by the DHI Group was applied to simulate the salinity level changes in the YRE. The model was based on a flexible unstructured mesh approach, and had been previously used for applications in coastal and estuarine environments [18]. The system was based on the numerical solution of the 2D incompressible Reynolds averaged Navier–Stokes equations, with assumptions made for the Boussinesq and hydrostatic pressures. The spatial discretization of the governing equations were performed using an element-centered finite volume method. The spatial domain was discretized by the subdivision of the continuum into non-overlapping elements. In the 2D model, the elements could be triangular or quadrilateral [19].

### 2.3.1. Governing Equations

The following equations, the conservation of mass and momentum integrated over the vertical, describe the flow and water level variations:

Continuity equation:

$$\frac{\partial \zeta}{\partial t} + \frac{\partial p}{\partial x} + \frac{\partial q}{\partial y} = \frac{\partial d}{\partial t} \tag{1}$$

Momentum equation:

$$\frac{\partial p}{\partial t} + \frac{\partial}{\partial x}\left(\frac{p^2}{h}\right) + \frac{\partial}{\partial y}\left(\frac{pq}{h}\right) + gh\frac{\partial \zeta}{\partial t} + \frac{gp\sqrt{p^2+q^2}}{C^2 h^2} - \frac{1}{\rho_w}\left[\frac{\partial}{\partial x}\left(h\tau_{xx}\right) + \frac{\partial}{\partial y}\left(h\tau_{xy}\right)\right] - \Omega q - fVV_x + \frac{h}{\rho_w}\frac{\partial}{\partial x}(p_a) = 0 \tag{2}$$

$$\frac{\partial p}{\partial t} + \frac{\partial}{\partial y}\left(\frac{q^2}{h}\right) + \frac{\partial}{\partial x}\left(\frac{pq}{h}\right) + gh\frac{\partial \zeta}{\partial t} + \frac{gp\sqrt{p^2+q^2}}{C^2 h^2} - \frac{1}{\rho_w}\left[\frac{\partial}{\partial y}\left(h\tau_{yy}\right) + \frac{\partial}{\partial x}\left(h\tau_{xy}\right)\right] - \Omega q - fVV_y + \frac{h}{\rho_w}\frac{\partial}{\partial y}(p_a) = 0 \tag{3}$$

Symbol list: $d$ is still water depth; $\zeta$ is surface elevation ($h = \zeta + d$); $p,q$ is unit-width discharge in the $x$ and y directions (m/s); $C$ is Chezy's coefficient; $f$ is wind resistance coefficient; $V$ is wind speed; $V_x$, $V_y$ is current velocity in the $x$ and y directions (m/s); $\Omega$ is Coriolis parameter; $p_a$ is atmospheric pressure; $\tau_{xx}$, $\tau_{xy}$, $\tau_{yy}$ is effective shear stress in the different directions [20].

Salinity variations were simulated by MIKE 21 AD (advection–dispersion module), which solves so-called advection–dispersion equation for dissolved or suspended substances in two dimensions (this is in fact the mass-conservation equations):

$$\frac{\partial}{\partial t}(hc) + \frac{\partial}{\partial x}(uhC) + \frac{\partial}{\partial y}(vhC) = \frac{\partial}{\partial x}\left(hD_x\frac{\partial c}{\partial x}\right) + \frac{\partial}{\partial y}\left(hD_y\frac{\partial c}{\partial y}\right) - FhC = S \qquad (4)$$

2.3.2. Boundary Conditions and Parameter Settings

1. *Boundary Conditions*

The space domain of the model was as follows: upstream to the Jiangyin Station in Jiangsu Province, at approximately 200 km away from the Xu River in the YRE. The offshore had three open boundaries in the south, north, and east, respectively. The spatial extent of the model was from 29.5° N to 32.5° N in the S–N direction, and from 120° E to 124.5° E in the W–E direction, with a total area of 93,185 km$^2$. The topographical river data were measured. Then, the sea area data were digitalized to an underwater topographical sea chart. The computational domain was composed of an unstructured triangular mesh with 54,243 nodes and 92,771 elements. The largest mesh was located at the eastern ocean boundary, and the smallest was located in the North Passage. Generally speaking, the mesh size decreased from the open sea to the near shore (Figure 4). Then, based on the results of previous tests of mesh sensitivity, the differences in the physical factors were computed using mesh lengths from 200 to 8000 m.
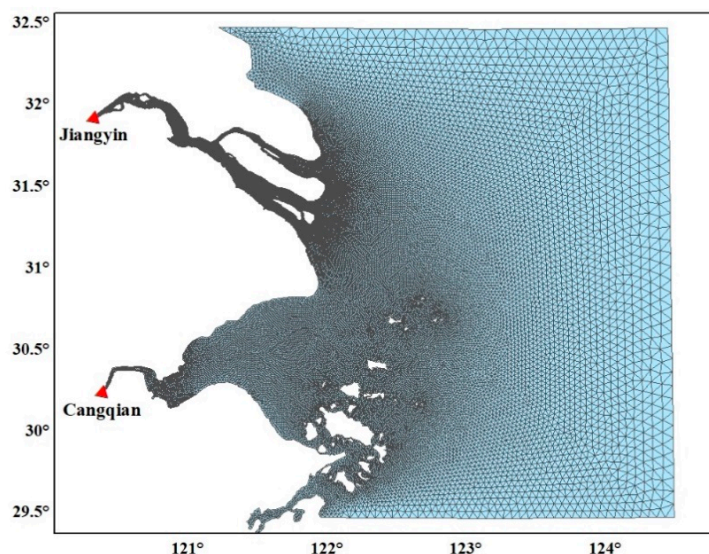


**Figure 4.** The compitational mesh of Yangtze River Estuary.

The land boundary of the model required the conditions of "non-importable and slippery". That is to say, the flow velocity was zero along the normal direction of the closed boundary. In the open sea areas, a tidal wave model was used to calculate the tide levels of the three outer boundaries of the outer sea. In this study, the global tidal wave model TPXO6.2 [21,22] was selected. The open boundary varies with time. The initial tidal level and velocity are defined as 1 m and 0 m/s, respectively.

According to the flow correlation analysis between Datong and Jiangyin stations [23], the runoff processes of the two stations were found to be similar. Therefore, the discharge data of the Datong station was selected as the flow boundary of Jiangyin. The flow boundary of Cangqian was determined to be 1000 m$^3$/s. During the experimental process, dry and wet grids were used to discriminate the model shoals. The values of hdry = 0.005 m, hflood = 0.05 m, and hwet = 0.1 m were utilized for each parameter [20].

The salinity value of the upper reaches of the model was 0, and salinity levels of 15‰ to 30‰ were linear interpolation from west to east in the southern boundary; a 35‰ salinity linear interpolation was determined in the northern boundary from west to east, using a 25‰ to 35‰ salt content as the

linear interpolation. The salinity field obtained from the initial salinity 0 (continuous for 3 months) was used as the initial salinity field of the model [24].

*2.  Parameters*

The time step was $\Delta t$ = 30 s.  The horizontal viscossity coefficient was calculated using Smagorinsky's formula, and the vortex viscosity was estimated based on the velocity gradient [24]. It was found that the roughness field had major impacts on the tides.  In this study, the roughness was repeatedly calibrated according to the depth of the different regions.  The range of roughness (n) was between 0.0105 and 0.02.  The salinity horizontal diffusion coefficient was observed to have a certain influence on the salinity field of the Yangtze Estuary. It was found that the greater the diffusion coefficient, the faster the salinity diffusion, and the greater the diffusion range.  Therefore, based on this study's repeated calculations and calibrations, the salinity diffusion coefficient was set as a constant value of 100 m$^2$/s [25–27].

### 2.3.3. Validation of the Numerical Model

The computing time for model is from 00 a.m. 11 February 2002 to 00 a.m. 13 March 2002, which lasted for a month. The validation time of the model is from 00 a.m., 1 March 2002 to 00 a.m. 10 March 2002. In this paper, four tidal station data of Chongmingzhou (Cmz), Lianxinggang (Lxg), Nanmen (Nm), and Hengsha (Hs) are selected for tide level verification (Figure 5).
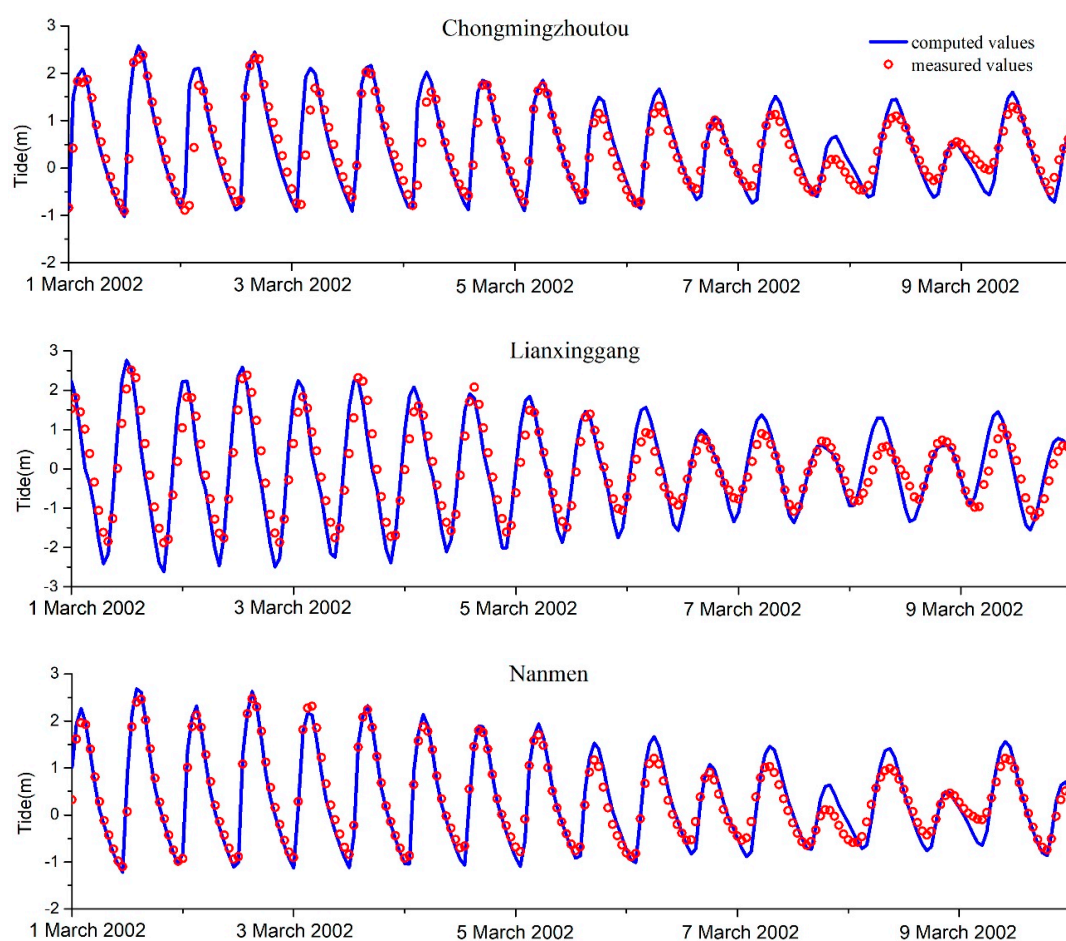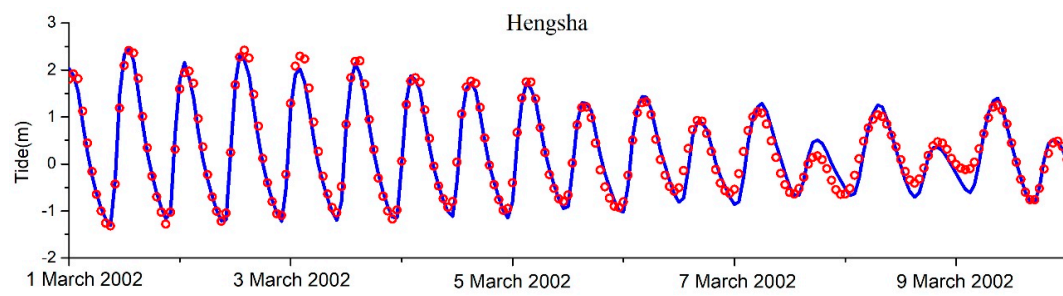
**Figure 5.** *Cont.*

**Figure 5.** Verification of tidal level.

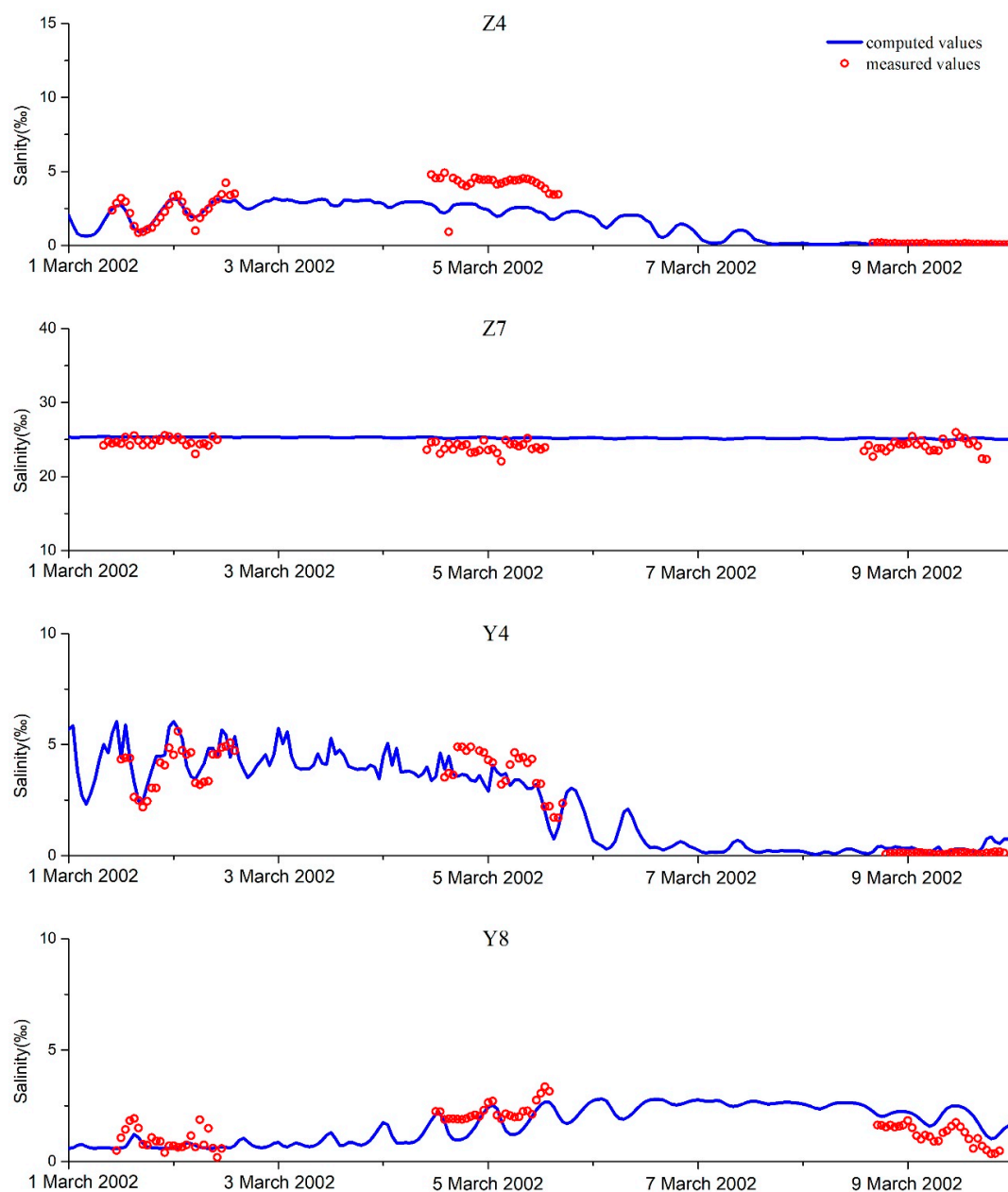Four salinity tests of Z4, Z7, Y4 and Y8 were selected for salinity verification (Figure 6).



**Figure 6.** Verification of salinity levels.

Model results are quantitatively assessed against the observed values using the skill model [28]. The skill model is as below:

$$skill = 1 - \frac{\Sigma_{i=1}^{N}|M-D|^2}{\Sigma_{i=1}^{N}(|M-\bar{D}|+|D-\bar{D}|)^2} \tag{5}$$

Symbol list: *M* is the measured values; *D* is the mean value of in situ observed data; a skill value of 1.0 indicates perfect agreement between the model results and observed data, excellent for skill between 0.65 and 1, very good for skill in the range of 0.5–0.65, good for skill in the range of 0.2–0.5, and poor for skill less than 0.2.

The numerical model was validated at 4 tide stations (Cmz, Lxg, Nm, and Hs) and 4 salinity stations (Z4, Z7, Y4 and Y8) around the YRE spanning the period from March 1, 2002 to March 10, 2002 (for positions see Figure 1). The time series of the hourly measured data at 8 stations are collected to validate the simulations. The simulation results at Cmz, Lxg, Nm, Hs, Z4, Z7, Y4 and Y8 are in excellent agreement with the observations (Figures 5 and 6). The skill values are 0.94, 0.92, 0.95, 0.91, 0.71, 0.81, 0.79 and 0.77 at eight stations (Table 2).

**Table 2.** Root-mean-square error (RMSE) and skill values of each validation.

| Tidal Station | Cmz | Lxg | Nm | Hs | Salinity Station | Z4 | Z7 | Y4 | Y8 |
|---|---|---|---|---|---|---|---|---|---|
| RMSE | 0.51 | 0.56 | 0.61 | 0.54 | RMSE | 0.69 | 0.66 | 0.68 | 0.63 |
| Skill | 0.94 | 0.92 | 0.95 | 0.91 | Skill | 0.71 | 0.81 | 0.79 | 0.77 |

From the verification results, the skill of tidal level simulation is above 0.9, and the fitting effect is very good. The skill of salinity level simulation is 0.71–0.81, which is slightly lower than the fitting result of the tide level. This is because, when at low tide, some stations have extremely low salinity and high sensitivity to water flow, so some of the measurements have deviations from the measured salinity.

## 3. Results

### 3.1. Changes in the Salinity Levels Caused by the River Discharges

The model was run for river discharges of 14,832 m$^3$/s, 16,331 m$^3$/s, 18,112 m$^3$/s and 27,856 m$^3$/s, respectively, at the Jiangyin boundary. The other conditions did not change. The salinity level changes at a total 14 selected stations (SB1-SB4, NB1, NB2, NC1, SC1, and T1–T6) were analyzed. As can be seen in Figure 1, the SB1 station was located at the upstream of the bifurcation point of the SB and NB; SB2–SB4 was located in the lower reach of the SB; NB1 and NB2 were located in the upper and lower reaches of the NB, respectively; NC1 was located in the middle reach of the NC; SC1 was in the lower reach of the SC; and T1–T6 stations were uniformly located in the offshore area.

Table 3 and Figure 7(1) show the mean salinity level of the NB with the different river discharges. The overall salinity level of the NB was observed to be in a high state. It was also indicated that the river discharge decreased, while the mean salinity level was generally increased from the upper reaches of the NB to the offshore. Moreover, the amplification in the upper reach was found to be higher than that in the lower reach and offshore. The amplification at station T1 was greater than that at station NB2. This was determined to be due to the fact the salinity level at the NB2 was mainly subjected to the runoff of the NB, the flow spilt ratio of which was observed to be very small at less than 1% [29]. Meanwhile, the salinity level at station T1 was exposed not only to the runoff from the NB, but also the runoff from the SB.
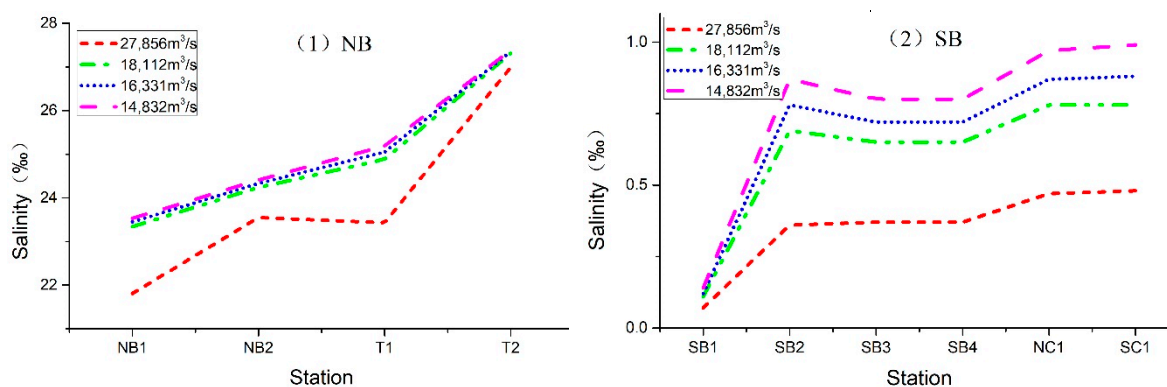
**Table 3.** Mean salinity level of the North Branch (NB) in different river discharges.

| Station | Mean Salinity Level with the Discharge of 27,856 m³/s (‰) | Mean Salinity Level and Amplification | | | | | |
| --- | --- | --- | --- | --- | --- | --- | --- |
| | | 18,112 m³/s | | 16,331 m³/s | | 14,832 m³/s | |
| | | Mean Salinity Level (‰) | Amplification (‰) | Mean Salinity Level (‰) | Amplification (‰) | Mean Salinity Level (‰) | Amplification (‰) |
| NB1 | 21.81 | 23.34 | 7.04 | 23.45 | 7.53 | 23.53 | 7.91 |
| NB2 | 23.55 | 24.24 | 2.95 | 24.33 | 3.33 | 24.41 | 3.65 |
| T1 | 23.43 | 24.88 | 6.22 | 25.05 | 6.94 | 25.19 | 7.52 |
| T2 | 26.99 | 27.31 | 1.18 | 27.35 | 1.33 | 27.38 | 1.45 |

Table 4 and Figure 7(2) present the mean salinity level of the SB under the different river discharges. With the decreasing of the river discharge, the mean salinity level was found to have significantly increased at a rate greater than that of the NB. The salinity of the South Branch was a "high–low–high" distribution. This is because the saltwater intrusions have two ways into the SB. One way is affected by the sea tides, and the other is the result of saltwater spilled over from NB. The amplification of the mean salinity level increased along the channel from stations SB1 and SB4 to stations NC1 and SC1. The T3 station was found to be mainly influenced by the runoff from the NC, while station T5 was determined to be obviously subjected to the runoff from the SB. Furthermore, the amplifications of mean salinity levels at stations T3 and T5 were found to be greater than those at stations T4 and T6, respectively, which indicated that there is a good response relationship between the mean salinity levels and river discharges.

**Table 4.** Mean salinity level of the South Branch (SB) in different river discharges.

| Station | Mean Salinity Level with the Discharge of 27,856 m³/s (‰) | Mean Salinity Level and Amplification | | | | | |
| --- | --- | --- | --- | --- | --- | --- | --- |
| | | 18,112 m³/s | | 16,331 m³/s | | 14,832 m³/s | |
| | | Mean Salinity Level (‰) | Amplification (‰) | Mean Salinity Level (‰) | Amplification (‰) | Mean Salinity Level (‰) | Amplification (‰) |
| SB1 | 0.07 | 0.11 | 61.77 | 0.12 | 81.40 | 0.14 | 104.04 |
| SB2 | 0.36 | 0.69 | 92.73 | 0.78 | 116.74 | 0.87 | 141.89 |
| SB3 | 0.37 | 0.65 | 77.45 | 0.72 | 97.43 | 0.80 | 118.53 |
| SB4 | 0.37 | 0.65 | 74.01 | 0.72 | 93.27 | 0.80 | 113.81 |
| NC1 | 0.47 | 0.78 | 67.73 | 0.87 | 86.66 | 0.97 | 107.28 |
| SC1 | 0.45 | 0.78 | 74.82 | 0.88 | 97.04 | 0.99 | 122.77 |
| T3 | 3.27 | 5.17 | 58.13 | 5.66 | 73.20 | 6.18 | 89.08 |
| T4 | 23.09 | 24.57 | 6.41 | 24.79 | 7.37 | 24.99 | 8.21 |
| T5 | 11.71 | 15.91 | 35.87 | 16.70 | 42.68 | 17.45 | 49.04 |
| T6 | 22.24 | 24.15 | 8.59 | 24.45 | 9.91 | 24.71 | 11.09 |



**Figure 7.** Mean salinity level of the selected stations in different river discharges.

*3.2. Correlation between the Salinity Levels and the River Discharges*

In order to determine the quantitative relationship between the river discharges and the salinity levels, the linear function (y = Ax + B) was used, as detailed in Figure 8 and Table 5.
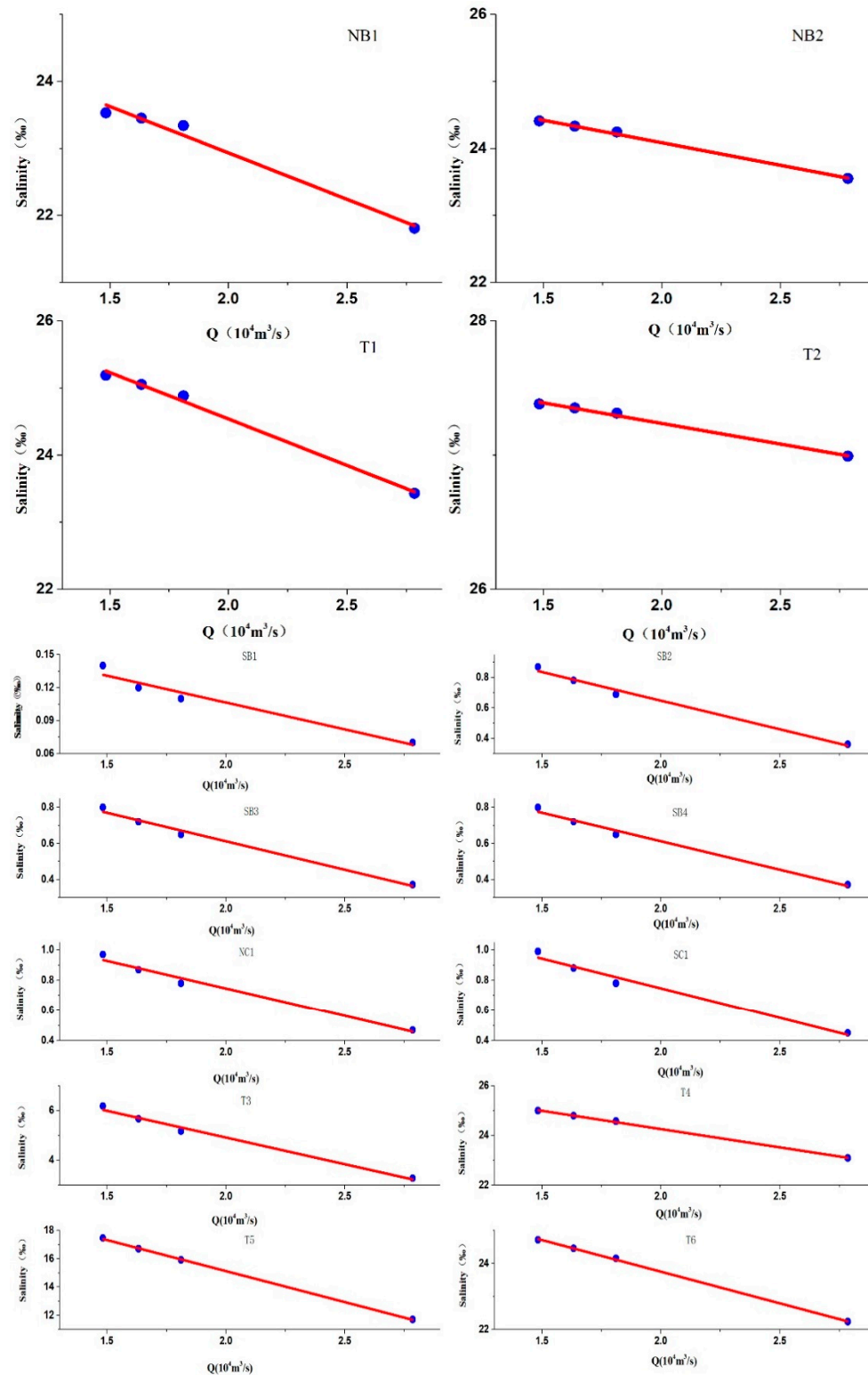


**Figure 8.** Correlation between the river discharge and sea level in the YRE and offshore area.

　　　The correlations between the river discharge and the mean salinity levels in the YRE and offshore were determined. It was found that the river discharge and the mean salinity levels had a notable positive correlation, with a correlation coefficient in the range of 0.971 to 1, which revealed the high precision of the fitting curves. The slope (coefficient A) of the curve could show the influence of the river discharge on the mean salinity levels. The slope was observed to generally decrease along the channel from station SB1 to station SC1. Meanwhile, the coefficient B increased. This indicated that the greater the distance from the offshore, the larger the impact of the river discharge; the lower the salinity value; and the weaker the change in salinity. In the upper reaches of the NB, the slope of the NB1 was the greatest with a value of −1.382, which indicated that the impacts of the runoff on the mean salinity levels of the NB1 were the largest in the NB and SB. Due to the generally high salinity in the NB, the slopes of the stations in the SB were lower than those in the NB. The salinity values of the T1, T3, and T5 were lower than those of the T2, T4 and T6, respectively, while the slopes were larger. This is due to the fact that the T2, T4, and T6 stations were located away from the estuary. Therefore, the runoff was weak, and the salinity values were high and stable.

**Table 5.** Statistics of coefficients in the linear expression of fitting curve in the NB and SB.

| Station | Coefficient A | Coefficient B | $R^2$ |
| --- | --- | --- | --- |
| NB1 | −1.382 | 25.697 | 0.973 |
| NB2 | −0.671 | 25.426 | 0.996 |
| T1 | −1.384 | 27.307 | 0.992 |
| T3 | −0.307 | 27.849 | 0.992 |
| SB1 | −0.049 | 0.204 | 0.973 |
| SB2 | −0.377 | 1.402 | 0.996 |
| SB3 | −0.317 | 1.246 | 0.992 |
| SB4 | −0.317 | 1.246 | 0.992 |
| NC1 | −0.365 | 1.475 | 0.928 |
| SC1 | −0.393 | 1.532 | 0.983 |
| T3 | −2.150 | 9.216 | 0.983 |
| T4 | −1.471 | 27.196 | 0.983 |
| T5 | −4.371 | 23.871 | 0.971 |
| T6 | −1.910 | 27.571 | 0.999 |

### 3.3. Spatial Distribution of the Salinity in the YRE and Its Offshore Areas

　　　The current study continued to carry out research on the spatial distribution of the salinity in the YRE and its offshore areas in order to better study the relationship between the changes in salinity and the river discharge. This part analyzes the salinity distribution, the change of salinity excessive area, and salinity amplification lines under different conditions in the YRE. The Chinese drinking water standard requires that the salinity of raw water should be less than 0.45‰. The Chinese drinking water standard requires that the salinity of raw water should be less than 0.45‰.

　　　Figure 9 illustrates the space distribution of the salinity during the spring tides. The salinity of the NB was observed to have a high concentration. Also, it was observed that under the spring tide conditions in the SB, when the discharge was 27,856 m³/s, the salinity of the SB was lower than 0.45‰, and no saltwater instrusion was evident. However, as the runoff decreased, the salinity standard was gradually exceeded in the SB, and the influence of the saltwater intrusions gradually became aggravated.

　　　The driving force in the tide under the action of the saltwater intrusion that can cover the area gradually increases with the increase of tidal strength, and the river discharge has played an important role in the resistance to saltwater intrusion. The saltwater intrusion is the process of interaction between a driving force (tide level) and impedance resistance (river discharge), and the process conforms to the principle of volume energy accumulation and impedance [1].
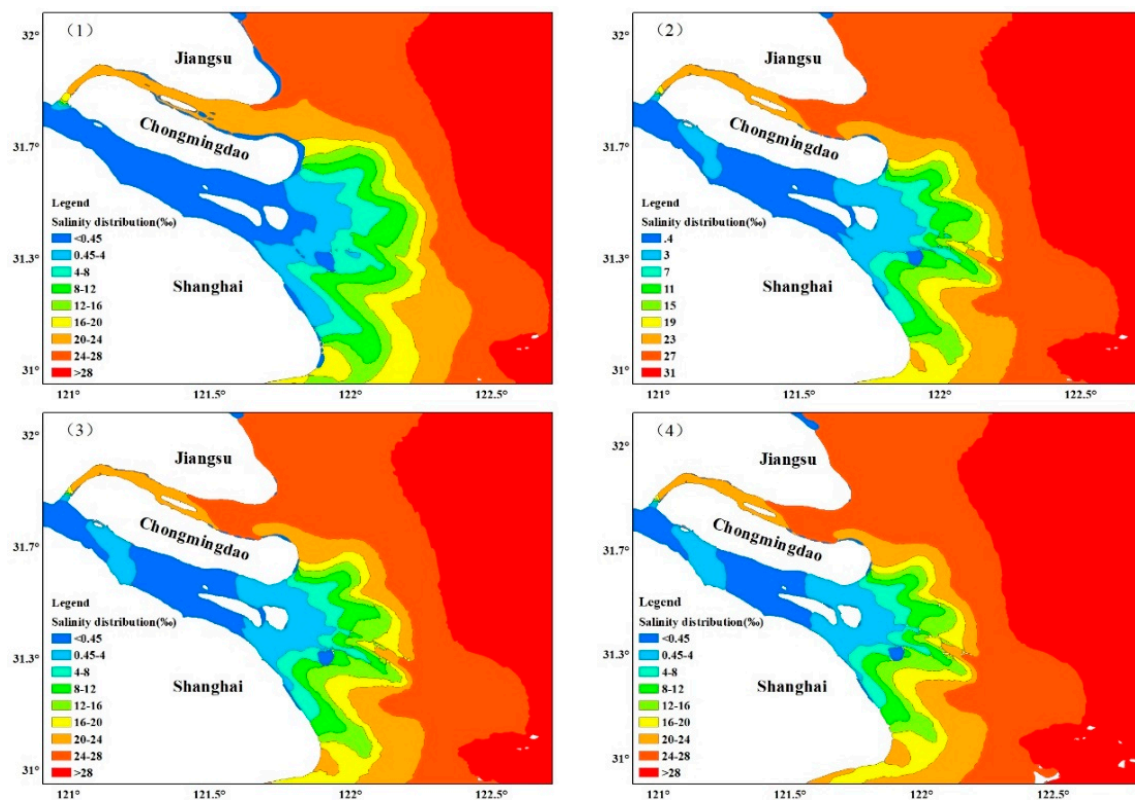
**Figure 9.** The space distribution of salinity in the spring tide: (**1**) Q = 27,856 m$^3$/s; (**2**) Q = 18,112 m$^3$/s; (**3**) Q = 16,331 m$^3$/s; (**4**) Q = 14,832 m$^3$/s.

Figure 10 shows the trends of the salinity changes in the YRE and its offshore areas at the neap tide, which were similar to those detailed in Figure 8. Furthermore, under the same discharge conditions, the excess areas of salinity during the spring tide periods were larger than those during the neap tide. Since the tides are the driving force of the salt water intrusions, it was found that the more intense the tides, the more severe the salt water intrusions. It was also observed that when the runoff decreased, the saltwater became backcropped in the NB, which resulted in increased saltwater intrusions in downstream areas. The excess salinity areas in the upper reaches of the SB, as well as in the downstream sections of the area, continuously increased and expanded into the middle reach region.
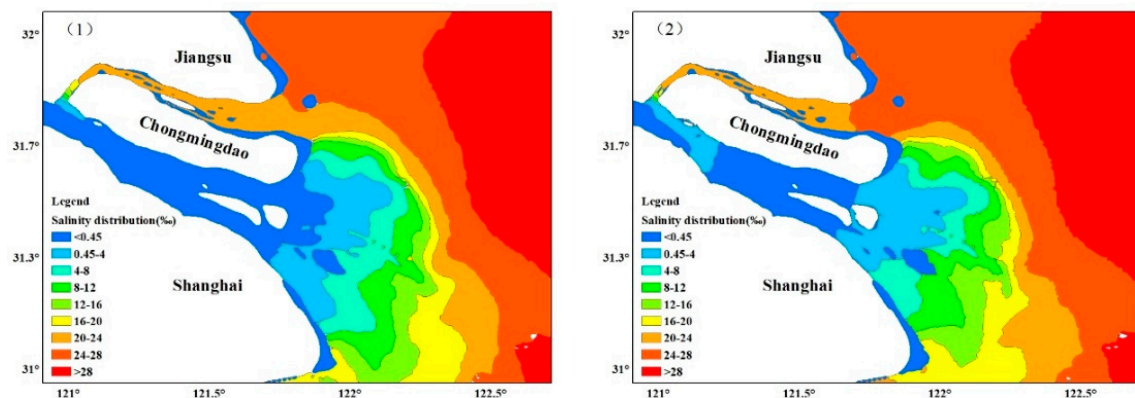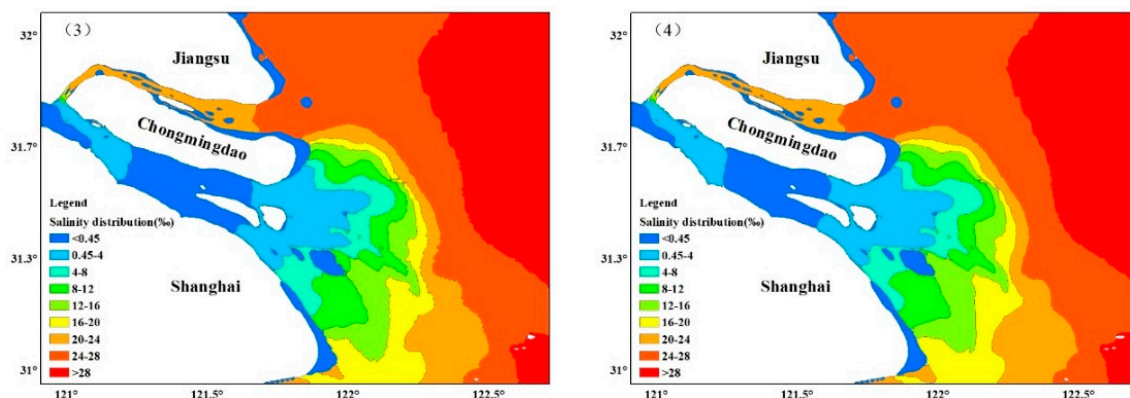


**Figure 10.** *Cont.*

**Figure 10.** The space distribution of salinity in the neap tide: (**1**) Q = 27,856 m$^3$/s; (**2**) Q = 18,112 m$^3$/s; (**3**) Q = 16,331 m$^3$/s; (**4**) Q = 14,832 m$^3$/s.

Since the intakes of the Three Great Reservoirs (Changxing Reservoir, Qingcaosha Reservoir, and Dongfeng Xisha Reservoir) in the YRE are all on the south branch [16], and the north branch is in high salinity for a long time, this part analyzes the salinity changes of the south branch of the YRE.

Since the intakes of the Three Great Reservoirs (Chenhang Reservoir, Qingcaosha Reservoir, and Dongfeng Xisha Reservoir) in the YRE are all on the South Branch [16], and the North Branch is in high salinity for a long time, this part focuses on analyzing the distribution of salinity in the SB. As can be seen in Table 6, when the discharge was 27,856 m$^3$/s, regardless of the type of tide present, the excess area percentage of the SB was less than 10%. However, when the discharge was reduced to 16,331 m$^3$/s, the excess salinity areas rapidly increased, and the percentage reached over 50%. Therefore, the size of the discharge had a significant impact on the salt water intrusions.

**Table 6.** Excess area and percentage of salinity at spring tide and neap tide in different river discharges in the SB.

| Tide (m) | 27,856 m$^3$/s | | 18,112 m$^3$/s | | 16,331 m$^3$/s | | 14,832 m$^3$/s | |
|---|---|---|---|---|---|---|---|---|
| | Excess Area (km$^2$) | Percentage (%) | Excess Area (km$^2$) | Percentage (%) | Excess Area (km$^2$) | Percentage (%) | Excess Area (km$^2$) | Percentage (%) |
| Spring tide | 115 | 8 | 588 | 41 | 761 | 53 | 890 | 62 |
| Neap tide | 14 | 1 | 531 | 37 | 718 | 50 | 847 | 59 |

Figure 11 details the differences in the salinity levels between the different river discharges and the multi-year river discharge (27,856 m$^3$/s) during the dry seasons. When the river discharge decreased, the mean salinity levels inside the estuary rapidly increased. The salinity in the NB had been in a high concentration state and was less affected by the runoff. The salinity levels remained relatively stable, and the amplification lines were unchanged. The salinity in the upper and lower reaches of the SB were observed to have increased significantly. The amplification line (0.2‰) was extended from the upstream and downstream areas to the middle reach area. The amplification line of 0.45‰ near the entrance of the YRE extended upstream, oppressing the amplification line of 0.2‰. The amplification line of 2‰ was mainly concentrated within a 40 km range of the entrance, and interactions between the river discharges and the tides were evident. The range of the salinity changes was found to be relatively stable. However, when moving away from the entrance to the estuary, the effects of the runoff were observed to weaken. For example, the amplification lines were gradually reduced.
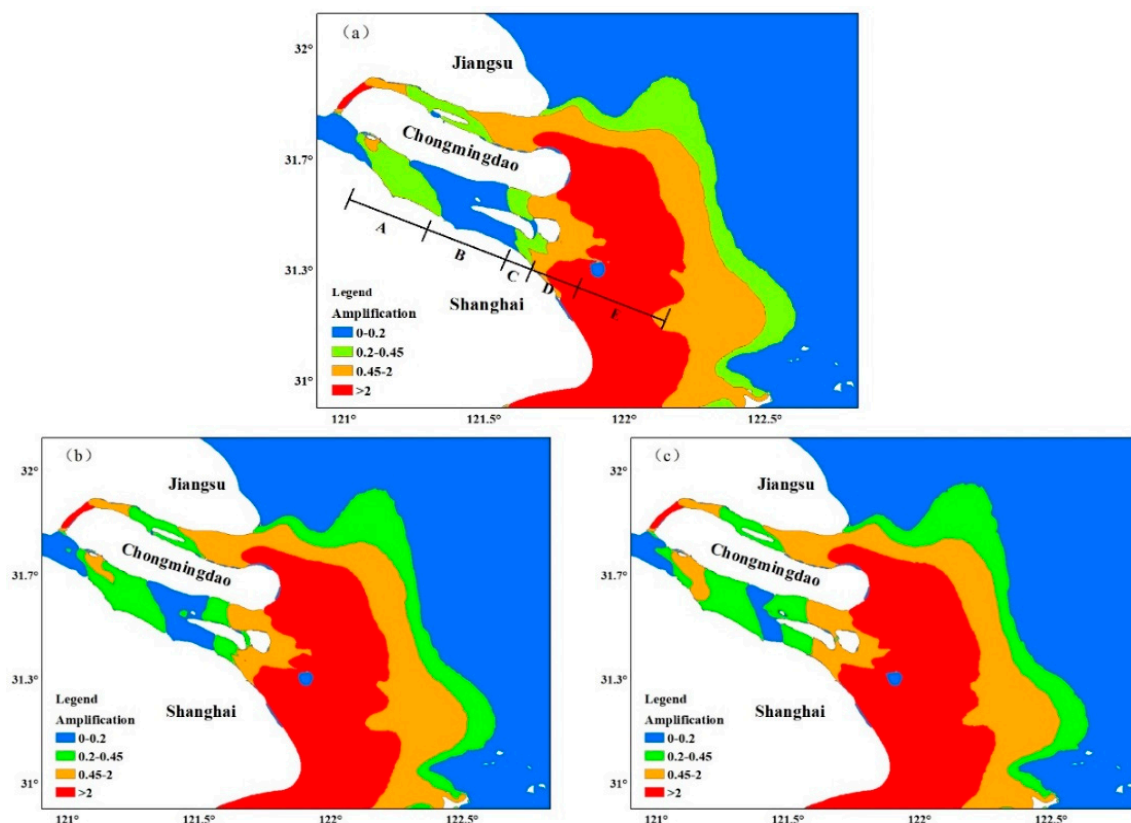
**Figure 11.** Differences of salinity level between different river discharges and multiyear river discharge in the dry season: (**a**) Q = 18,112 m$^3$/s; (**b**) Q = 16,331 m$^3$/s; (**c**) Q = 14,832 m$^3$/s; A, B, C, D and E are the length of salinity amplification (unit: km).

Table 7 details the lengths of the salinity amplification in the SB and offshore areas compared to the multi-year discharge of 27,856 m$^3$/s. In Figure 10, A, B, C, D, and E represent the respective lengths of the different salinity variations. As the discharges decreased, the length of B (<0.2‰) gradually narrowed. When the runoff was reduced to 14,832 m$^3$/s, the length was shortened from 27.94 km to 6 km. As the river discharges decreased, the lengths of A, C, D, and E were observed to gradually rise, and the total length increased by approximately 3 km. These data show that not only the river discharge, but also the high salinity which spills over from the NB, influence the salinity change in the upper reaches of the SB.

**Table 7.** The length of salinity amplification in the SB and offshore (unit: km).

| Discharge (m$^3$/s) | Total | A (0.2–0.45‰) | B (<0.2‰) | C (0.2–0.45‰) | D (0.45–2‰) | E (>2‰) |
|---|---|---|---|---|---|---|
| 18,112 | 113.27 | 24.96 | 27.94 | 8.63 | 18.05 | 33.69 |
| 16,331 | 115.26 | 29.20 | 17.31 | 11.33 | 20.22 | 37.20 |
| 14,832 | 116.19 | 33.60 | 6.00 | 14.57 | 22.59 | 39.43 |

The impact of river discharge on saltwater intrusion is mainly reflected in the SB and offshore areas. As the distance from the mouth of the YRE is getting farther, the effect of the river discharge gradually weakens, and there is basically no effect at the end.

### 3.4. Influences of the River Discharges on the Four Reservoirs in the YRE

It has been determined that the four freshwater reservoirs in the YRE are often affected by saltwater intrusions, especially during the dry seasons. The saltwater intrusions in the SB were mainly

caused by two factors: saltwater spilled over from the NB to the SB; and the occurrences of saltwater intrusions during the periods of low levels of river discharge. Due to the reduction in runoff during dry seasons, and the increased human water usage, the low river discharges aggravated the saltwater intrusions, and negatively influenced the effective operations of the reservoirs.

In the study, the salinity change process of four reservoirs under different flow rates through the model was simulated. Figure 12 shows that as the river discharges decreased, the salinity of the reservoir exceeded the standard. The changes in the salinity levels in the Dongfeng Xisha Reservoir displayed large fluctuations, and at times exceeded the standard. In comparison with the Dongfeng Xisha Reservoir major fluctuations, the salinity of the other reservoirs changed relatively slowly. When the river discharge was 27,856 m$^3$/s, part of the Dongfeng Xisha Reservoir exceeded time limit. However, the salinity levels of the remaining three reservoirs were found to be below 0.45‰, and were not affected by the salt water intrusions. This was due to the fact that the Dongfeng Xisha Reservoir was located at the junction of the SB and NB. In this location, interactions occurred between the highly concentrated saltwater and the river water as it entered the sea. Therefore, the salinity levels fluctuated greatly.
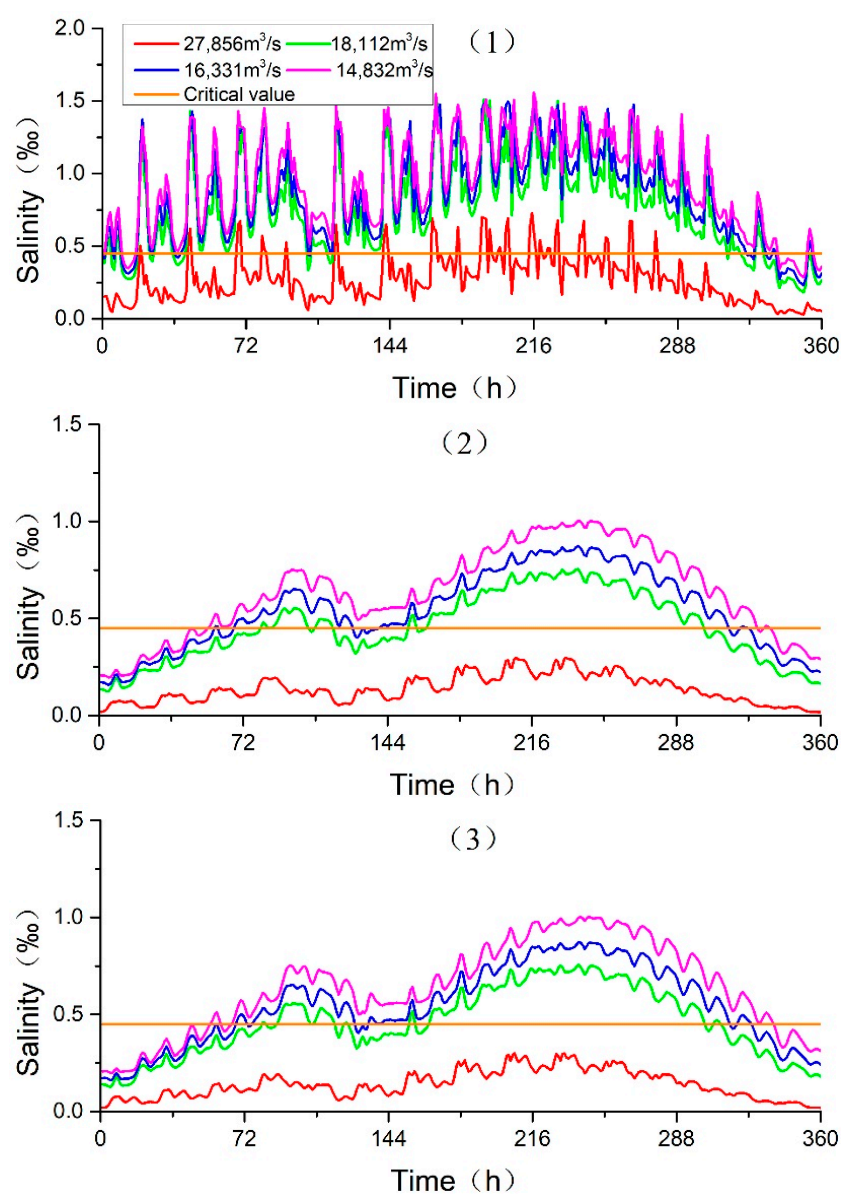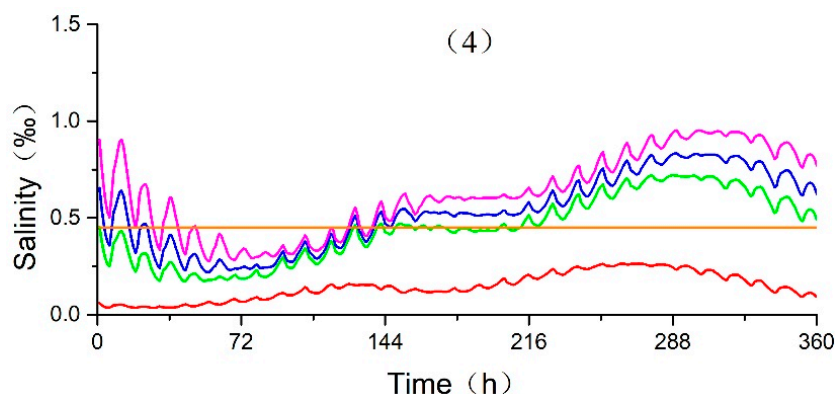


**Figure 12.** *Cont.*

**Figure 12.** The salinity changes of four freshwater reservoirs in different river discharge: (**1**) Dongfengxisha; (**2**) Baogang; (**3**) Chenhang; (**4**) Qingcaosha.

Table 8 presents the monthly mean percentages of the salinity increases in the discharges of the three rivers compared with the average annual river discharges. The Dongfeng Xisha Reservoir was located farthest away from the open sea, and was found to be dominated by the saltwater spilling over from the NB to the SB. Since the Dongfeng Xisha Reservoir was located at the junction of the SB and NB, the interactions between the highly concentrated saltwater and the river as it entered the sea resulted in major fluctuations in the salinity levels. The salinity amplification at the Dongfeng Xisha Reservoir was approximately twice that of the Chenhang and Baogang Reservoirs. The Baogang and Chenhang Reservoirs were located close to each other, and the salinity increasing percentages were observed to be similar. Due to its closeness to the sea, it was found that the Qingcaosha Reservoir's increasing percentage was relatively small.

**Table 8.** Monthly mean salinity increasing percentage in different river discharge.

| Discharge ($m^3/s$) | Dongfengxisha | Baogang | Chenhang | Qingcaosha |
| --- | --- | --- | --- | --- |
| 18,112 | 177.08% | 61.42% | 62.41% | 58.91% |
| 16,331 | 216.50% | 91.51% | 92.33% | 88.27% |
| 14,832 | 256.77% | 123.99% | 124.50% | 121.36% |

In Table 9, it can be seen that the increasing percentage totals and the longest successive times of the salinity exceeded 0.45‰ at the four examined freshwater reservoirs during the river discharges in a typical month (31 days or 745 h). It was found that when it was 18,112 $m^3/s$, the river discharge started to exert influences on the water intake at the Dongfeng Xisha Reservoir resulting in the longest successive time that exceeded 0.45‰ and reached 196 h, with the total excess time correspondingly increasing to 614 h. It was also determined that when the discharge was 16,331 $m^3/s$, the increasing longest successive time exceeded 0.45‰ at the Dongfeng Xisha Reservoir and reached 204 h, which was more than that at the Chenhang (175 h) and Baogang (203 h) Reservoirs. The impacts of the river discharges on the increasing time exceeding 0.45‰ at the Dongfeng Xisha Reservoir was greater than at the other reservoirs. The salinities at the four reservoir locations exceeded the drinking water standard for more than 23 days in the 14,832 $m^3/s$ river discharge scenario, and had major negative effects on the water intake in the YRE.

**Table 9.** The increasing total and the longest successive time of salinity exceeding 0.45‰ at four reservoirs in the four scenarios in a typical month (unit: h).

| Discharge (m$^3$/s) | Dongfengxisha | | Baogang | | Chenhang | | Qingcaosha | |
|---|---|---|---|---|---|---|---|---|
| | Total | Successive | Total | Successive | Total | Successive | Total | Successive |
| 27,856 | 93 | 4 | 0 | 0 | 0 | 0 | 0 | 0 |
| 18,112 | 614 | 196 | 360 | 133 | 453 | 154 | 364 | 157 |
| 16,331 | 655 | 204 | 496 | 175 | 556 | 203 | 500 | 275 |
| 14,832 | 686 | 318 | 572 | 266 | 608 | 283 | 552 | 316 |

## 4. Discussion

### 4.1. Salinity Levels in the North Branch (NB) and South Branch (SB)

The NB is crucial for the saltwater intrusions into the YRE. The high salinity not only affects the freshwater usage on Chongming Island along the NB of Jiangsu Province, but also affects the water withdrawn of the SB (Dongfeng Xisha Reservoir). During the dry seasons, the salinity of the NB still remains above 20‰ even though the tide levels are low [30,31]. However, the data were found to be lacking regarding these limits. In addition, strong salt intrusions may also occur during the flood seasons. From 18 to 19 September of 2001, the freshwater discharges from the Yangtze River were observed to be high (38,000 m$^3$/s) at Datong station. However, the saltwater intrusions into the NB remained strong, and were even recorded to have affected the water intake levels on the southern coast of Shanghai at the Chenhang Reservoir [32]. This situation had never occurred before. The saltwater intrusions had two ways into the SB. One way was affected by the sea tides, and the other was the result of spill-over conditions. The salinity levels in the SB were distributed from upstream to downstream as "high–low–high". The "high" point was located at the north and south junction at Chongming Island, and the "low" point was located near the central Wusongkou. The excess salinity areas (salinity > 0.45‰) were in the upper reaches of the SB, in which the downstream part of the area continuously increased and expanded toward the middle reach area (Figures 9 and 10).
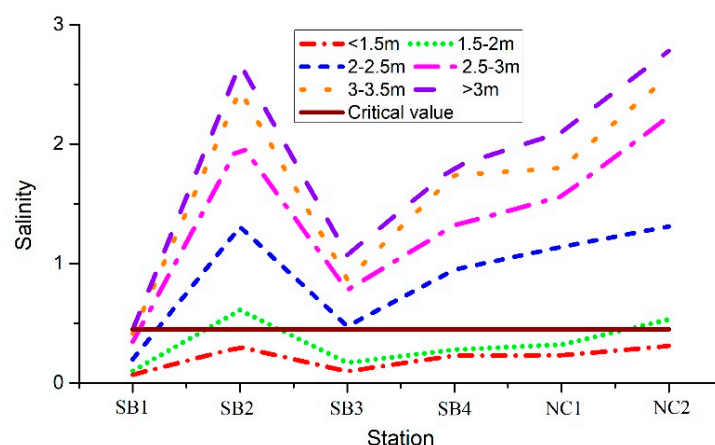
### 4.2. Tidal Distributions

It is known that the impacts of the tides on the saltwater intrusions in estuaries are also important factors. Tides are astronomical phenomena which are cyclically affected by the phases of the moon, and tend to be the driving forces of saltwater intrusions [33]. In the YRE, the tides have size and period variations within half-monthly cycles. The salinity levels of the YRE also display one-level and one-half cycle variations [34]. In the eigenvalues which reflect the intensity levels of the tides, the tidal ranges have been found to be more objective in reflecting the characteristics of tide intensities [35]. It has been observed that when the tidal range is higher, the larger tide levels move farther forward, resulting in higher levels of saltwater intrusions until finally the maximum level of salinity is reached [36].

Table 10 and Figure 13 show that under the average river discharge of the dry seasons (16,542 m$^3$/s) at Datong station, the mean salinity levels of the selected stations of the SB displayed different tidal ranges as follows: <1.5 m; 1.5 to 2 m; 2 to 2.5 m; 2.5 to 3 m; 3 to 3.5 m; and >3.5 m. It was observed that at the same rate of flow, as the tidal range increased, the salinity levels of each station continuously increased. From upstream to downstream along the SB, the stations generally showed rising trends. The salinity of the SB was found to be distributed as "high-low-high". These results were consistent with those of the previous related studies.

**Table 10.** Mean salinity level of the SB in different tidal range under average river discharge of dry season.

| Station | Mean Salinity Level with Different Tide Range (‰) | | | | | |
|---|---|---|---|---|---|---|
| | <1.5 m (‰) | 1.5–2 m (‰) | 2–2.5 m (‰) | 2.5–3 m (‰) | 3–3.5 m (‰) | >3.5 m (‰) |
| SB1 | 0.070 | 0.101 | 0.198 | 0.343 | 0.412 | 0.445 |
| SB2 | 0.301 | 0.610 | 1.307 | 2.324 | 2.610 | 2.870 |
| SB3 | 0.098 | 0.170 | 0.475 | 0.778 | 0.868 | 1.072 |
| SB5 | 0.230 | 0.279 | 0.949 | 1.320 | 1.740 | 1.810 |
| NC1 | 0.231 | 0.321 | 1.140 | 1.560 | 1.800 | 2.100 |
| SC1 | 0.310 | 0.532 | 1.310 | 2.230 | 2.570 | 2.780 |



**Figure 13.** Mean salinity level of the selected stations in different tidal range.

### 4.3. Topography of the Area

The topography of a study area is the most important boundary condition for any model. In this research study, the measured topography data from 2002 of the Yangtze River Estuary were used. In the estuary of the Yangtze River, in addition to its natural evolution, two other channels exist which are known to be greatly affected by human activities. These channels are the NB and SB. Between the 1950s and 1990s, due to the closure of the shoal and deposition of the river bed (particularly [37] in the upper reaches), the terrain of the North Branch had undergone major changes. These changes led to the river discharge becoming greatly reduced. Also, the tidal ranges in the upper reaches of the river, along with the saltwater intrusions, were increased during that period [38]. However, since 2000, the NB has been less affected by human activities, which has resulted in fewer changes in the area's topography [37,39]. Another major human activity in the NB was that a deep-water channel was dredged and reinforced in 1998. This was completed in order to increase the water depth to ensure the safety of the fairways. The Eastern WDP (south to north project) caused a decrease of the river discharges, and resulted in an enhancement of the salt-water intrusions. In particular, the sand bars around the river mouth were found to have experienced notable increases in their salinity levels [40].

## 5. Conclusions

In this study, the effects of river discharges on the saltwater intrusions in the YRE were explored. The effects were examined using a hydrodynamic and salinity transport numerical model with high-resolution unstructured grids, and spatial variabilities in bottom roughness. The 25%, 50%, and 70% frequencies of the river discharges during the dry seasons were determined to be 18,112, 16,331, and 14,832 $m^3/s$, respectively, and the multi-year averaged river discharge was 27,856 $m^3/s$. These river discharge values were used to simulate the salinity level changes caused by the different river discharges. The main findings of this study are summarized as follows.

The salinity levels of the selected stations in the NB showed slowly decreasing trends from the upstream to the downstream, and the salinity was maintained above 20‰. The salinity of the SB was distributed as "high–low–high", and the changes in the salinity levels were greatly affected by the river discharges. When compared with the average river discharge scenario, the increases in the salinity under the other flow conditions were determined to be above 60%.

The salinity levels rose as the river discharges decreased, and the amplification line of the SB was greater than that on the NB. The salinity levels displayed very good positive correlations with the river discharges in the YRE, with a correlation coefficient range of between 0.971 and 1.

When the river discharge was 27,856 m$^3$/s, the standard rate of salinity was exceeded. However, in the SB, it was found to be always lower than 10% regardless of the tide levels. The SB was impacted less by the salt water intrusions. However, when the runoff was reduced to 16,331 m$^3$/s, the standard salinity rate became exceeded in the SB, and reached more than 50%. At this point, the saltwater intrusion was considered to be at a serious level.

The mean salinity inside the SB rapidly increased when the river discharge decreased. The amplification line of 0.2‰ continued to shrink, and the amplification lines of 0.45‰ and 2‰ gradually expanded. In the areas far away from the river's entrance to the sea, the effects of runoff were weak, such as the amplification lines became gradually reduced.

The changes in the river discharges were found to have significant impacts on the freshwater reservoir water withdrawal. The salinity levels at the Dongfeng Xisha Reservoir were mainly affected by the salinized water spilling over from the NB. The amplifications of the monthly mean salinity at the Dongfeng Xisha Reservoir were observed to be larger than at the Chenhang, Baogang, and Qingcaosha Reservoirs in the three river discharge scenarios of this study. When the river discharge was maintained at 27,856 m$^3$/s, the salinity levels of the Baogang, Chenhang, and Qingcaosha Reservoirs all remained below 0.45‰. The salinity levels at the four reservoir locations were observed to have exceeded the drinking water standard for more than 23 days in the 14,832 m$^3$/s river discharge scenario, which potentially negatively affected the drinking water of the population living near the YRE.

**Author Contributions:** Conceived the study, Z.X.; Data curation, Z.X. and Y.H.; Software, Z.X. and W.D.; Supervision, G.Y.; Writing-original draft, Z.X.; Writing-review & editing, J.M. and H.W.

## References

1.  Chen, M.-J.; Hu, Y.-J.; Ma, J.; Yan, L.; Zhou, F.; Wang, Y. Diffusion response function and preliminary application of saltwater intrusion in the Yangtze River Estuary. *Adv. Water Sci.* **2017**, *28*, 203–212. (In Chinese)
2.  Zhang, E.; Savenije, H.H.G.; Wu, H.; Kong, Y.; Zhu, J. Analytical solution for salt intrusion in the Yangtze Estuary, China. *Estuar. Coast. Shelf Sci.* **2011**, *91*, 492–501. [CrossRef]
3.  Bhuiyan, M.J.A.N.; Dutta, D. Assessing impacts of sea level rise on river salinity in the gorai river network, Bangladesh. *Estuar. Coast. Shelf Sci.* **2012**, *96*, 219–227. [CrossRef]
4.  Yuan, Y.R.; Liang, D.; Rui, H.X. The numerical simulation and analysis of three-dimensional seawater intrusion and protection projects in porous media. *Sci. China* **2009**, *52*, 92–107. [CrossRef]
5.  Chen, S.L.; Zhang, E.F.; Guo-Chuan, G.U.; Ping, L.I. Salt intrusion in the south passage of Yangtze River Estuary during extraordinary dry year. *Mar. Sci. Bull.* **2009**, *28*, 29–36.
6.  Wang, W. Reduction effect of runoff and tide upon estuarine and bay channel geographical evolution-examples of Shenquan Channel and Wukan Channel. *Mar. Sci.* **1992**, *06*, 54–57.

7.　Kuang, C.; Chen, W.; Gu, J.; Su, T.-C.; Song, H.; Ma, Y.; Dong, Z. River discharge contribution to sea-level rise in the Yangtze River Estuary, China. *Cont. Shelf Res.* **2017**, *134*, 63–75. [CrossRef]

8.　Wu, H.; Zhu, J.; Chen, B.; Chen, Y. Quantitative relationship of runoff and tide to saltwater spilling over from the North Branch in the Changjiang Estuary: A numerical study. *Estuar. Coast. Shelf Sci.* **2006**, *69*, 125–132. [CrossRef]

9.　Xue, P.; Chen, C.; Ding, P.; Beardsley, R.C.; Lin, H.; Ge, J.; Kong, Y. Saltwater intrusion into the Changjiang River: A model-guided mechanism study. *J. Geophys. Res.* **2009**, *114*. [CrossRef]

10.　Wu, H.; Zhu, J. Advection scheme with 3rd high-order spatial interpolation at the middle temporal level and its application to saltwater intrusion in the Changjiang Estuary. *Ocean Model.* **2010**, *33*, 33–51. [CrossRef]

11.　Li, L.; Zhu, J.; Wu, H.; Guo, Z. Lateral saltwater intrusion in the north channel of the Changjiang Estuary. *Estuar. Coasts* **2013**, *37*, 36–55. [CrossRef]

12.　Tang, J.-H.; Xu, J.-Y.; Zhao, S.-W.; Liu, W.-Y. Research on saltwater intrusion of the south branch of the Changjiang Estuary based on measured data. *Resour. Environ. Yangtze Basin* **2011**, *20*, 677–684. (In Chinese)

13.　Zhu, J.R.; Hui, W.U.; Lu, L.I.; Wang, B. Saltwater intrusion in the changjiang estuary in the extremely drought hydrological year 2006. *J. East China Normal Univ.* **2010**, *32*, 1–11.

14.　Chen, J.; Xu, H. Impacts of the yangtze river threegorge hydroengineering works on the Yangtze Estuaky. *Pesources Enuiron. Yangtza Valley* **1995**, *03*, 242–246.

15.　Chen, J.; Zhu, J.R. Sources for saltwater intrusion at the water intake of Qingcaosha Reservoir in the Changjiang Estuary. *Acta Oceanol. Sin.* **2014**, *36*, 131–141.

16.　Chen, L.; Zhu, J.R.; Wang, B. Research on Statistical Model of Saltwater Intrusion of Chenxing Reservoir in the Yangtze River Estuary. *Water Wastewater Eng.* **2013**, *49*, 162–165.

17.　Xu, M.J.; Yu, L.; Zhao, Y.W.; Li, M. The simulation of shallow reservoir eutrophication based on MIKE21: A case study of Douhe Reservoir in North China. *Procedia Environ. Sci.* **2012**, *13*, 1975–1988. [CrossRef]

18.　Hakim, B.A.; Wibowo, M.; Kongko, W.; Irfani, M.; Hendriyono, W.; Gumbira, G. Hydrodynamics modeling of giant seawall in Semarang Bay. *Procedia Earth Planet. Sci.* **2015**, *14*, 200–207. [CrossRef]

19.　Chubarenko, I.; Tchepikova, I. Modelling of man-made contribution to salinity increase into the Vistula Lagoon (Baltic Sea). *Ecol. Model.* **2001**, *138*, 87–100. [CrossRef]

20.　Dean, W.; Yuchen, S.; Jinxian, P. Study on activities and concentration of saline groupin the south branch in Yangtze River Estuary. *Procedia Eng.* **2015**, *116*, 1085–1094. [CrossRef]

21.　Egbert, G.; Bennett, A.F.; Foreman, M. Topex/poseidon tides estimated using a global inverse model. *J. Geophys. Res.* **1995**, *99*, 24821–24852. [CrossRef]

22.　Egbert, G.D.; Erofeeva, S.Y. Efficient inverse modeling of barotropic ocean tides. *J. Atmos. Ocean. Technol.* **2002**, *19*, 183–204. [CrossRef]

23.　Kuang, C.; Chen, W.; Gu, J.; He, L. Response of offshore sea level to river discharge in flood season in Yangtze Estuary. *Tongji Daxue Xuebao/J. Tongji Univ.* **2015**, *43*, 1266–1272.

24.　Shao, Y.; Wu, D.; Pan, J. Study on impact of runoff on saltwater intruding from the north branch in the Changjiang Estuary. *Procedia Eng.* **2015**, *116*, 824–833.

25.　Yang, T.J.; Wang, Y.G.; Huang, H.M.; Yuan, C.G. Research on salinity intrusion in the Yangtze River Estuary by numerical simulation. *J. Waterway Harbor* **2013**, *34*, 473–481.

26.　Feng, J. Application of MIKE21FM Numerical Model in Environmental Impact Assessment of ocean Engineering. Master's Thesis, Ocean University of China, Qingdao, China, 2011.

27.　Kuang, C.; Tang, L.; Chen, W.; Gu, J. Prediction and analysis of the impacts on wave in the Yangtze River Estuary due to potential sea level rise. *J. Tongji Univ.* **2016**, *44*, 1377–1383.

28.　Willmott, C. On the validation of models. *Phys. Geogr.* **1981**, *2*, 184–194.

29.　Zhang, Z.L.; Wei, R.; Liu, G.P.; Qiu, Z.Y.; Chen, P.; Min, F.Y. Recent river regime evolution of the north branch of the Yangtze River Estuary and development research of navigational channel resources. *Ocean Eng.* **2009**, *27*, 96–103.

30.　Zheng, J.M.; Yan, Y.L.; Chu, Y.L. Three dimensional baroclinic numerical model for simulating fresh and salt water mixing in the Yangtze Estuary. *China Ocean Eng.* **2002**, *16*, 227–238.

31.　Gong, Z. Three-dimensional baroclinic numerical model of current and salinity in Yangtze Estuary. Ph.D. Thesis, Hohai University, Nanjing, China, 2002.

32.　Shen, H.T.; Mao, Z.C.; Zhu, J.R. *Saltwater Intrusion in the Mouth of the Yangtze River*; Ocean Publishing: Plymouth, UK, 2003.

33. Gong, W.; Wang, Y.; Jia, J. The effect of interacting downstream branches on saltwater intrusion in the Modaomen Estuary, China. *J. Asian Earth Sci.* **2012**, *45*, 223–238. [CrossRef]

34. Ding, L.; Dou, X.P.; Gao, X.Y.; Hai-Dong, X.U.; Jiao, J. Analysis of saltwater intrusion into Yangtze Estuary during dry seasons of 2013 and 2014. *Hydro-Sci. Eng.* **2016**, *04*, 47–53.

35. Yang, Z.Y.; Cheng, H.Q.; Li, J.F. Nonlinear advection, coriolis force, and frictional influence in the south channel of the Yangtze Estuary, China. *Sci. China Earth Sci.* **2015**, *58*, 429–435. [CrossRef]

36. Chen, C.-S.; Liu, H.-D.; Beardsley, R.C. An unstructured, finite-volume, three-dimensional, primitive equation ocean model: Application to coastal ocean and estuaries. *J. Atmos. Ocean. Technol.* **2003**, *20*, 159–186. [CrossRef]

37. Zhu, J.-R.; Wu, H. Numerical simulation of the longest continuous days unsuitable for water intake in the Dongfengxisha Reservoir of the Changjiang Estuary. *J. East China Normal Univ.* **2013**, *28*, 1–8.

38. Chen, B.C. The change of the general form and the transport of the water, load and salt about the north-branch of the Changjiang River mouth. *Chin. Geogra. Sci.* **1996**, *65*, 21. [CrossRef]

39. Chen, W.; Chen, K.; Kuang, C.; Zhu, D.Z.; He, L.; Mao, X.; Liang, H.; Song, H. Influence of sea level rise on saline water intrusion in the Yangtze River Estuary, China. *Appl. Ocean Res.* **2016**, *54*, 12–25. [CrossRef]

40. Xu, K.; Zhu, J.; Gu, Y. Impact of the eastern water diversion from the south to the north project on the saltwater intrusion in the Changjiang Estuary in China. *Acta Oceanol. Sin.* **2012**, *31*, 47–58. [CrossRef]